Spectrochimica Acta Part A: Molecular and Biomolecular Spectroscopy 133 (2014) 307–317

Contents lists available at ScienceDirect

Spectrochimica Acta Part A: Molecular and Biomolecular Spectroscopy

journal homepage: www.elsevier.com/locate/saa

Structural investigation of a self-assembled monolayer material 5-[(3-methylphenyl) (phenyl) amino] isophthalic acid for organic light-emitting devices

E. Babur Saş [a], M. Kurt [a,*], M. Can [b], S. Okur [c], S. İçli [d], S. Demiç [c]

[a] Department of Physics, Ahi Evran University, Kırsehir, Turkey
[b] Department of Engineering Sciences, Faculty of Engineering, Izmir Katip Celebi University, Cigli, 35620 Izmir, Turkey
[c] Izmir Katip Çelebi University, Material Science and Engineering, Çiğli, Izmir, Turkey
[d] Ege University, Solar Energy Institute, 35040 Bornova, Izmir, Turkey

HIGHLIGHTS

- Molecular structure of 5-[(3-methylphenyl) (phenyl) amino] isophthalic acid was studied.
- The FT-IR, Raman, NMR and UV–vis spectra of studied molecule were compared with calculated spectra.
- The vibrational frequencies were calculated by DFT method and discussed.
- The complete assignments are performed on the basis of the potential energy distribution (PED).

GRAPHICAL ABSTRACT

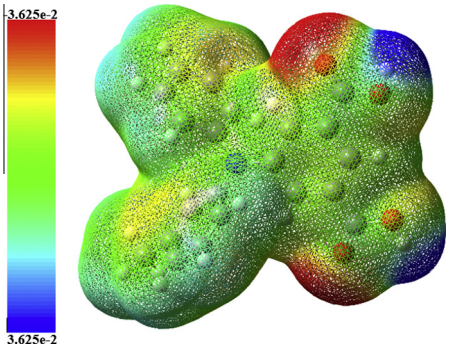

ARTICLE INFO

Article history:
Received 12 March 2014
Received in revised form 1 May 2014
Accepted 9 May 2014
Available online 20 May 2014

Keywords:
5-[(3-Methylphenyl) (phenyl) amino] isophthalic acid (MePIFA)
DFT
FT-IR
FT-Raman
Dispersive Raman
UV and NMR spectra

ABSTRACT

The molecular structure and vibrations of 5-[(3-methylphenyl) (phenyl) amino] isophthalic acid (MePIFA) were investigated by infrared and Raman spectroscopies, UV–Vis, ^{1}H and ^{13}C NMR spectroscopic techniques and NBO analysis. FT-IR, FT-Raman and dispersive Raman spectra were recorded in the solid phase. ^{1}H and ^{13}C NMR spectra and UV–Vis spectrum were recorded in DMSO solution. HOMO–LUMO analysis and molecular electrostatic potential (MEP) analysis were performed. The theoretical calculations for the molecular structure and spectroscopies were performed with DFT (B3LYP) and 6-311G(d,p) basis set calculations using the Gaussian 09 program. After the geometry of the molecule was optimized, vibration wavenumbers and fundamental vibration wavenumbers were assigned on the basis of the potential energy distribution (PED) of the vibrational modes calculated with VEDA 4 program. The total (TDOS), partial (PDOS) density of state and overlap population density of state (OPDOS) diagrams analysis were made using GaussSum 2.2 program. The results of theoretical calculations for the spectra of the title compound were compared with the observed spectra.

Introduction

TPD known as a triarylamine compound with two triphenylamine (TPA) moieties is widely used in organic light-emitting diodes (OLEDs) as hole-transport material [1–10]. The structure of

* Corresponding author. Tel.: +90 386 280 45 25; fax: +90 386 252 80 54.
E-mail address: kurt@gazi.edu.tr (M. Kurt).

http://dx.doi.org/10.1016/j.saa.2014.05.021
1386-1425/

TPA molecules with nitrogen atom is planar. This means, that the nitrogen atom and the three carbon atoms covalently bonded to the nitrogen atom are in the same plane [11–17]. The development of organic light-emitting diodes (OLEDs) has progressed due to their potential applications in many fields [16–18]. Multilayer OLEDs are known as one of the potential technologies for the next generation flat-panel display devices [18,19]. Multilayer OLED are fabricated as sandwich like structures between an indium tin oxide (ITO) anode and a metal cathode with an electron-transporting material (ETM) layer, a hole-transporting material (HTM) layer inside [18].

In this work, the spectroscopic approach of 5-[(3-methylphenyl) (phenyl) amino] isophthalic acid (MePIFA) molecule was investigated. The structure of molecule was optimized with DFT/B3LYP 6-311G(d,p). Infrared and Raman spectra were calculated and vibrational assignments were performed based upon potential energy distributions (PED). NMR and UV absorption spectra were recorded and compared with theoretically obtained spectra in DMSO. Additionally, HOMO LUMO and natural bond orbital (NBO) analysis were also carried out for MePIFA by DFT. Besides the total density of states (TDOS or DOS), the partial density of states (PDOS) and overlap population density of states (OPDOS) spectra of molecule were calculated using GaussSum 2.2 [20].

Experimental

The title compound was synthesized for the first time by Okur et al. [21]. The compound MePIFA in solid form were prepared using a KBr disc technique. The infrared spectrum of the compound was recorded in the range of 4000–600 cm^{-1} on a Perkin–Elmer FT-IR system spectrum BX spectrometer. The spectrum was recorded at room temperature, with a scanning speed of 10 cm^{-1} min^{-1} and the spectral resolution of 4.0 cm^{-1}. The Raman spectra of the compound were recorded between 3500–40 cm^{-1} with a Thermo Fisher Scientific model DXR dispersive Raman instrument using 532 and 780 nm laser excitation. FT-Raman spectrum of MePIFA did not provide any spectra. An InGaAs detector was used at room temperature. One hundred scans were collected with 4 cm^{-1} resolution by using a laser power of 100 mW. The ultraviolet absorption spectra of sample solved in DMSO was examined between 200 nm and 1100 nm with resolution of 1 nm by using Princeton Instrument Model of Acton Advanced SP2300A with two monochromator, UV–Vis recording spectrometer. The sample spectrum was taken inside a quartz tupe with DMSO. NMR experiments were performed in Bruker at 300 K. Chemical shifts were reported in ppm relative to tetramethylsilane (TMS) for ^1H and

Table 1
Same selected vibrational frequencies of MePIFA molecule.

No	Experimental wavenumber			Theoretical wavenumber				PED[a] (⩾10%)
	FT-IR	Dispersive Raman		Scaled[b]	I_{IR}	S_{Ra}	I_{Ra}	Assignments
		532 nm	780 nm					
9			63w	61	0.51	7.60	52.33	δCCN(39) + ΓCCCC(21)
10			86m	122	0.46	0.45	0.88	δCCC(67)
15			214w	206	3.78	4.71	3.68	ΓCCCC(55) + ΓCCCH(11) + ΓCCNC(15)
16		221w		230	1.96	6.80	4.40	δCCN(22) + ΓCCCC(51) + ΓCCNC(11)
21		333vw		340	3.68	5.16	1.80	υCC(48) + δCCC(22) + δOCO(18)
34				591	1.95	7.98	1.23	γOH[ΓCCOH(85)]
39	642vw	640vw		636	47.52	7.84	1.08	δCCC(35) + ΓCCCC(16) + γOH[ΓCCOH(11)]
43	696m	702vw		693	37.07	2.66	0.32	ΓCCCC(34) + ΓCCCH(28) + ΓCCNC(16)
46	758w			759	19.70	1.14	0.12	ΓCCCC(28) + ΓCCCH(30) + ΓCNCH(19)
48			776vw	776	4.90	3.41	0.35	ΓCCCC(11) + ΓCCCH(41) + ΓOCOC(19)
55	902vw			905	2.16	0.12	0.01	ΓCCCC(20) + γCH[ΓCCCH(73)]
57	935vw			930	0.84	2.93	0.23	γCH[ΓCCCH(77)]
60			950vw	952	0.10	0.23	0.02	ΓCCCC(20) + γCH[ΓCCCH(79)]
65			994m	983	12.63	36.65	2.66	υCC(26) + δCCC(59)
66		998vs		1007	72.10	5.77	0.41	υCC(18) + δCCC(27) + δCCH(10) + ΓCCCH(16)
69		1060vw		1069	9.38	1.05	0.07	υCC(45) + δCH[δCCH(44)]
78	1166vw			1164	184.96	22.86	1.29	υCC(30) + δCH[δCCH(18)] + δCOH(24)
79		1218vw		1206	48.77	125.46	6.72	υCC(34) + υCN(20) + δCCC(12) + δCH[δCCH(13)]
80				1238	40.18	19.22	0.99	υCC(19) + δCH[δCCH(63)]
81				1255	36.60	49.19	2.47	υCC(50) + υCN(14) + δCH[δCCH(22)]
83	1273vs			1279	77.91	72.76	3.55	υCC(27) + υCN(24) + δCCC(11) + δCCH(30)
84		1292vw		1289	29.17	28.52	1.37	υCC(52) + υCN(11) + δCCH(17)
88	1321m			1316	45.59	19.83	0.93	υCO(14) + δOCO(12) + δOH[δCOH(33)]
89		1340vw		1354	487.22	79.57	3.55	υCC(28) + υCO(14) + δCCC(12) + δOCO(10) + δCOH(20)
93	1428m			1429	37.32	4.88	0.20	υCC(48) + δCCC(10) + δCCH(26)
94				1441	16.18	2.78	0.11	υCC(32) + δCCC(11) + ρCH[δCCH(40)]
95				1442	7.76	13.76	0.55	ρCH[δHCH(53)] + ΓCCCH(14)
96	1452m			1452	18.56	2.76	0.11	υCC(14) + δCCH(12) + δHCH(53) + ΓCCCH(14)
98	1493m			1474	110.92	15.70	0.61	υCC(14) + δCCC(18) + δCCH(58)
103	1587s		1586w	1585	64.59	98.52	3.36	υCC(61) + δCCC(17) + δCCH(16)
104		1594m		1593	13.70	145.90	4.94	υCC(46) + δCCC(16) + δCCH(18)
105	1688vs			1742	509.80	21.19	0.61	υCO(84)
106		2027vw	2230w	1747	56.13	122.68	3.50	υCO(84)
107	2656w	2918vw		2924	29.38	231.36	2.03	υCH(100)
108	2863w			2977	18.66	84.25	0.70	υCH(99)
109				3002	16.98	71.89	0.59	υCH(100)
110				3058	4.61	78.56	0.61	υCH(100)
111	3033w	3061vw		3060	3.45	35.34	0.27	υCH(100)
121			3185vw	3135	5.97	50.88	0.37	υCH(100)
122	3633vw		3380vw	3647	114.08	193.68	0.86	υOH(100)
123				3648	93.21	242.02	1.08	υOH(100)

[a] PED: potential energy distribution, ν; stretching, γ; out-of plane bending, δ; in-plane bending, τ; torsion, ρ; scissoring, φ; twisting, r; rocking.
[b] Scaling factor was used as 0.967.

^{13}C NMR spectra in DMSO. NMR spectra were obtained at the base frequency of 400 MHz for ^{13}C and ^{1}H nuclei.

Computational details

MePIFA molecule has been optimized by DFT/B3LYP 6-311G(d,p) method. Bond lengths, bond angles and vibrational wavenumbers were calculated with the same method and vibrational wavenumbers were presented with the scale factors. The Raman activities (S_{Ra}) were converted to relative Raman intensities (I_{Ra}) by using the following relationship and derived from the intensity theory of Raman scattering [22,23]:

$$I_i = \frac{f(v_0 - v_i)^4 S_i}{v_i[1 - \exp\left(\frac{hcv_i}{kT}\right)]} \quad (1)$$

where v_0 is the wavenumber of the exciting laser ($v_0 = 9398.5\ cm^{-1}$), v_i is the vibrational wavenumber of the ith normal mode and S_i is the Raman scattering activity of the normal mode v_i. f is a constant and equal to 10^{-12}. H, k, c and T are Plank and Boltzmann constant, the speed of light and the temperature in Kelvin, respectively. The vibration modes are assigned on the basis of PED computed by using VEDA 4 program [24].

After optimization of the molecule, ^{1}H and ^{13}C NMR chemical shifts were calculated using B3LYP with 6-311G(d,p) basis set by the GIAO method. These calculations were made in DMSO, water and gas phase with reference to TMS. Chemical shifts calculated in the DMSO solution are in agreement with the experimental data obtained from DMSO solution. UV–Vis spectra, excitation energies, absorption wavelength and oscillator strengths were calculated in gas phase with TD-DFT and CIS methods. Furthermore, the same parameters were calculated by using TD-DFT method including IEF-PCM, and CIS method. In both methods, DMSO and water solvents were taken into account. HOMO and LUMO energies were performed with TD-DFT method with 6-311G(d,p) basis set. The natural bonding orbitals (NBO) calculations [25] were done using

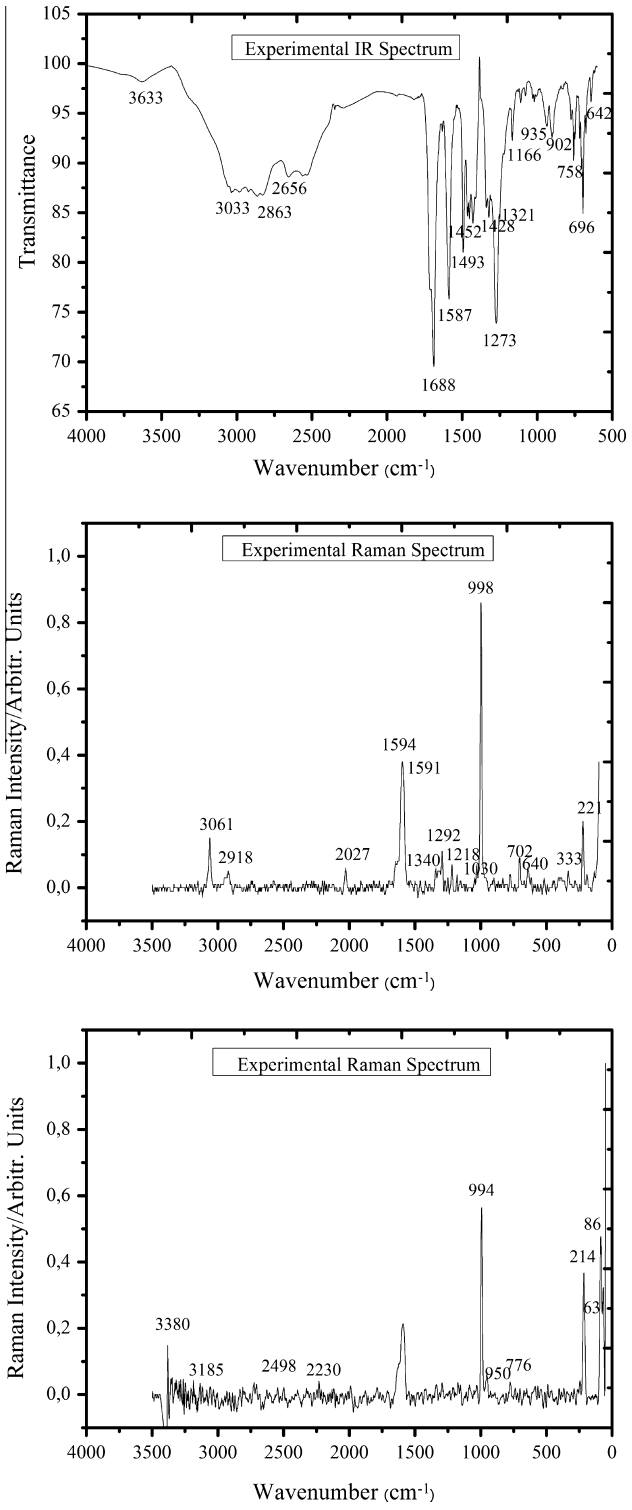

Fig. 1. The experimental infrared and Raman spectra of MePIFA.

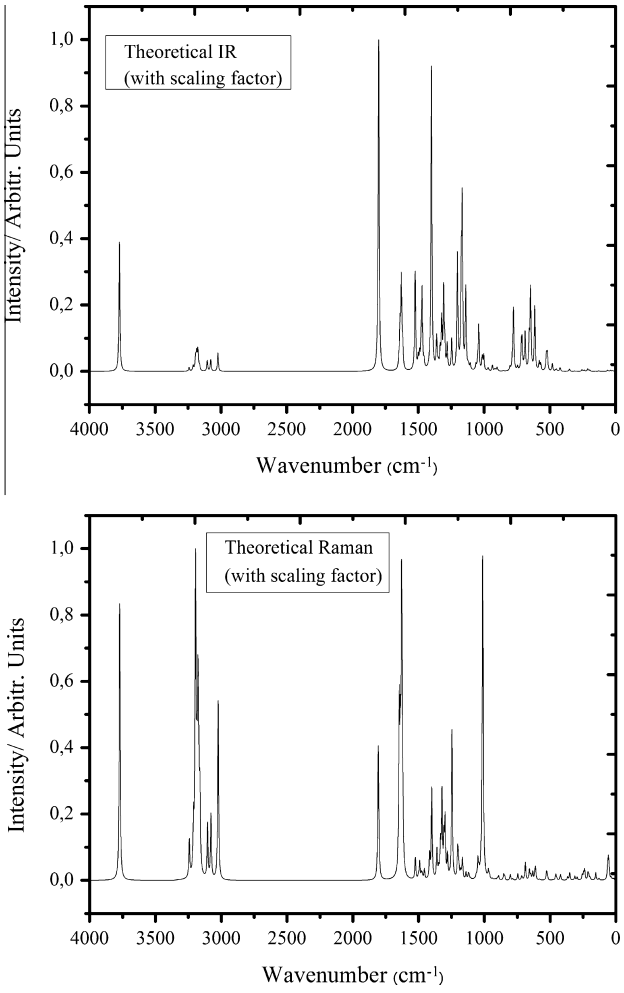

Fig. 2. The calculated infrared and Raman spectra of MePIFA.

the DFT/B3LYP 6-311G(d,p) method. Furthermore, GaussSum 2.2 program were used to obtain density of states (TDOS or DOS), the partial density of states (PDOS) and overlap population density of states (OPDOS) spectra [20]. The PDOS and OPDOS spectra were generated by convolution of the molecular orbital information with Gaussian curves of unit height and a FWHM (Full Width at Half Maximum) of 0.3 eV. All calculations were made on the personal computer using Gaussian 09 program package [26].

Result and discussion

Molecular geometry

The title molecule optimized with DFT/B3LYP/6-311G(d,p) method are shown in Fig. S1 (Supporting information) with its molecular geometry. Bond lengths and bond angles with X-ray data of triphenylamine were listed in Table S1 [27]. In this molecule, the central nitrogen and three adjacent carbon atoms are within the same plane. Torsional angles attached to nitrogen are N1—C2—C4—C7 = 179.92°, N1—C13—C14—C16 = 179.07^0 and N1—C23—C25—C28 = 179.45^0 for MePIFA. COOH and CH_3 groups are coplanar according to benzene ring in MePIFA molecule and torsional angles are C23—C24—C26—C32 = 179.998^0, C23—C25—C28—C36 = 179.97^0 and C13—C14—C16—C40 = 178.65^0. Bond angles of molecule between C2—N1—C23 and C13—N1—C23 are ∼120^0 and bond angle of C2—N1—C13 is ∼119^0.

The optimized bond lengths of the C—C bond in ring systems were calculated in the range of 1.387–1.410 Å for 2-fluorophenylboronic acid [28] and were observed 1.365 Å to 1.406 Å for 3–flurophenylboronic acid [29]. In this study, the same bond lengths were calculated at 1.39 Å. But, C2—C3, C2—C4, C23—C24 and C23—C25 bond lengths (1.40 Å) slightly longer than the rest of the substituents. Bond lengths of molecule between N1—C2 and N1—C13 are around ∼1.425 Å and bond length of N1—C23 is obtained as 1.411 Å.

Vibrational spectral analysis

MePIFA molecule with 43 atoms and 123 fundamental vibrational modes has C_1 symmetry. These fundamental vibrations are active in both IR and Raman. Vibrational spectral assignments were calculated with the B3LYP/6-311G(d,p) basis set and were

Table 2
Second order perturbation theory analysis of Fock matrix in NBO basis for MePIFA.

Donor (*i*)	Type	ED/e	Acceptor (*j*)	Type	ED/e	$E^{(2)a}$ (kJ mol^{-1})	$E(j)-E(i)^b$ (a.u)	$F(i,j)^c$ (a.u)
N1—C2	σ	1.98	N1—C13	σ*	0.04	2.21	1.17	0.046
			N1—C23	σ*	0.04	2.30	1.19	0.047
			C13—C14	π*	0.38	0.68	0.79	0.023
N1—C13	σ	1.98	N1—C2	σ*	0.04	2.21	1.17	0.046
			N1—C23	σ*	0.04	2.28	1.18	0.047
			C2—C4	σ*	0.03	1.73	1.33	0.043
			C2—C4	π*	0.39	0.64	0.79	0.022
N1—C23	σ	1.98	N1—C2	σ*	0.04	2.26	1.19	0.046
			N1—C13	σ*	0.04	2.26	1.19	0.046
			C2—C4	π*	0.39	0.55	0.80	0.021
			C13—C14	π*	0.38	0.53	0.81	0.020
C26—C32	σ	1.97	C23—C24	σ*	0.03	3.05	1.23	0.055
			C24—C26	σ*	0.02	1.97	1.24	0.044
C2—C3	σ	1.97	C2—C4	σ*	0.03	4.35	1.26	0.066
			C3—C5	σ*	0.02	3.54	1.28	0.060
C28—C36	σ	1.97	C23—C25	σ*	0.03	3.05	1.23	0.055
			C28—C30	σ*	0.02	2.42	1.24	0.049
C2—C4	σ	1.97	N1—C13	σ*	0.04	2.61	1.11	0.048
			C2—C3	σ*	0.03	4.35	1.26	0.066
			C4—C7	σ*	0.02	3.55	1.28	0.060
C2—C4	π	1.66	C3—C5	π*	0.33	19.01	0.29	0.067
			C7—C9	π*	0.34	21.01	0.29	0.070
C13—C14	σ	1.97	C13—C15	σ*	0.03	4.45	1.26	0.067
			C14—C16	σ*	0.02	4.35	1.28	0.067
C13—C14	π	1.66	C15—C18	π*	0.33	18.67	0.29	0.066
			C16—C20	π*	0.35	21.61	0.30	0.072
C16—C20	σ	1.97	C14—C16	σ*	0.02	3.87	1.27	0.063
			C16—C40	σ*	0.02	1.99	1.11	0.042
			C18—C20	σ*	0.02	3.44	1.27	0.059
C16—C20	π	1.65	C13—C14	π*	0.38	20.05	0.27	0.067
			C15—C18	π*	0.33	22.90	0.28	0.072
C23—C24	σ	1.97	C23—C25	σ*	0.03	4.33	1.26	0.066
			C24—C26	σ*	0.02	3.83	1.27	0.062
C23—C24	π	1.61	C25—C28	π*	0.36	22.26	0.29	0.072
			C26—C30	π*	0.37	19.61	0.29	0.067
C25—C28	π	1.64	C23—C24	π*	0.36	18.28	0.28	0.064
			C26—C30	π*	0.37	22.04	0.29	0.071
C26—C30	π	1.64	C23—C24	π*	0.36	22.31	0.28	0.071
			C25—C28	π*	0.36	19.24	0.29	0.066
N1	LP(1)	1.72	C2—C4	π*	0.39	16.96	0.28	0.063
			C13—C14	π*	0.38	16.05	0.28	0.061
			C23—C24	π*	0.36	25.01	0.27	0.075
O33	LP(2)	1.85	C26—C32	σ*	0.07	18.13	0.68	0.101
			C32—O34	σ*	0.10	32.55	0.61	0.128
O34	LP(2)	1.83	C32—O33	π*	0.24	43.88	0.35	0.112
O37	LP(2)	1.85	C28—C36	σ*	0.07	18.13	0.68	0.101
			C36—O38	σ*	0.10	32.54	0.61	0.128
O38	LP(2)	1.83	C36—O37	π*	0.24	43.90	0.35	0.112
C13—C14	π*	0.38	C16—C20	π*	0.35	273.40	0.01	0.085

performed with a detailed description of the normal modes based on the potential energy distribution (PED). The calculations were done in gas phase. The experimental data were obtained in solid form. The obtained theoretical wavenumbers (for some selected vibrational modes) are given together with the experimental results in Table 1 and Table S2 (whole data). The scaling factor of 0.967 was used to fit the calculated wavenumbers with the obtained experimental data. The experimental and calculated IR and Raman spectra were given in Fig. 1 and Fig. 2.

Ring vibrations

The ring C—C stretching vibrations occur between 1430–1625 cm^{-1}. In general, the bands are observed at the frequency ranges between 1625–1590, 1575–1590, 1470–1540, 1430–1465 and 1280–1380 cm^{-1} for five bands given by Varsanyi [30]. In the present work, aromatic C—C stretching vibrations were computed at the frequency ranges between 1593–1452, 1441–1408, 1354, 1314–1069 and 1015 cm^{-1} by using B3LYP/6-311G(d,p) method and they are observed at 1587, 1493, 1452, 1428, 1273, 1166 cm^{-1} and at 1594, 1586, 1340, 1292, 1218, 1060 cm^{-1} in FT-IR and dispersive Raman, respectively. The main C—C stretching vibrations are computed at 1314 and 1576 cm^{-1} with the PED contribution 63%. The results show that the C—C stretching vibrations modes are convoluted with the other vibrational modes. In plane and out-of-plane bending modes have been obtained by using B3LYP method and they show good agreement with the experimental wavenumbers. The results show that the PEDs of these modes are not pure as shown in Table 1.

Table 3
Experimental and calculated chemical shifts (ppm) of MePIFA.

Atom	Calculated			Experimental
	DMSO	Water	Gas	DMSO
C32	168.71	168.73	167.16	166.39
C36	168.68	168.70	167.14	166.39
C23	155.72	155.72	155.23	148.70
C2	154.50	154.50	154.36	146.53
C13	154.22	154.22	154.15	146.42
C16	146.31	146.32	145.14	139.90
C25	134.24	134.24	134.49	132.69
C24	133.99	133.98	134.23	132.69
C5	133.79	133.80	133.41	129.85
C28	133.38	133.39	133.26	129.72
C7	133.36	133.36	133.01	129.85
C26	133.34	133.34	133.22	129.72
C18	133.20	133.20	133.06	125.60
C14	130.85	130.85	130.84	125.46
C3	130.45	130.44	130.44	125.19
C4	128.78	128.79	128.65	125.19
C20	128.59	128.59	128.28	124.04
C9	127.74	127.74	127.33	122.80
C30	127.69	127.69	127.94	122.26
C15	126.10	126.10	126.28	125.46
C40	21.23	21.22	21.55	20.76
H31	8.29	8.29	8.27	8.47
H27	8.00	7.99	8.07	8.16
H29	7.99	7.99	8.06	8.13
H10	7.48	7.48	7.32	8.00
H11	7.47	7.47	7.32	7.62
H21	7.34	7.34	7.21	7.62
H8	7.27	7.28	7.16	7.62
H12	7.26	7.27	7.10	7.36
H22	7.10	7.10	6.94	7.24
H6	7.07	7.07	7.00	7.62
H19	7.05	7.05	6.96	7.12
H17	6.95	6.95	6.88	6.95
H35	6.10	6.11	5.40	13.2
H39	6.10	6.11	5.40	13.2
H41	2.51	2.51	2.49	2.43
H43	2.07	2.08	1.97	2.43
H42	2.03	2.03	1.96	2.43

COOH vibrations

The carboxylic acid vibrational bands of MePIFA contain C—O, C═O and O—H vibrational modes. The C═O stretching band of carboxylic acids appears strongly in the region between 1740 and 1660 cm^{-1} [31].This band depends on the physical state, electronic and mass effects of neighboring substituents, conjugations and intramolecular and intermolecular hydrogen bonding [32–35]. The C═O stretching mode is the strongest band in FT-IR and appears with diminished intensity in FT-Raman [36]. In this study, it was observed at 1688 cm^{-1} as a very strong band in FT-IR and it appears at 2027, 2230 cm^{-1} in the dispersive Raman spectrum. The same band was calculated as 1742 and 1747 cm^{-1} with B3LYP/6-311G(d,p) method. The C═O stretching mode is pure according to PED calculations.

OH hydroxyl group connecting the molecules has a strong absorbance in the region between 3550 and 3200 cm^{-1} according to the reference [34]. The O—H stretching vibration of MePIFA molecule was calculated as 3647 and 3648 cm^{-1} with B3LYP, as given in Table 1. These bands were observed at 3633 cm^{-1} in FT-IR and at 3380 cm^{-1} in dispersive Raman. The hydroxyl stretching vibrational mode is pure according to PED calculations.

In-plane bending vibration of O—H group appears in the region 1440–1260 cm^{-1} in the FT-IR spectrum [35,37]. But out-of-plane bending vibration of O—H group appears in the region between 280 and 312 cm^{-1} for free O—H and in the region between 600 and 720 cm^{-1} for associated O—HO—H [38]. In-plane bending vibration of the molecule was calculated as 1316 cm^{-1} and

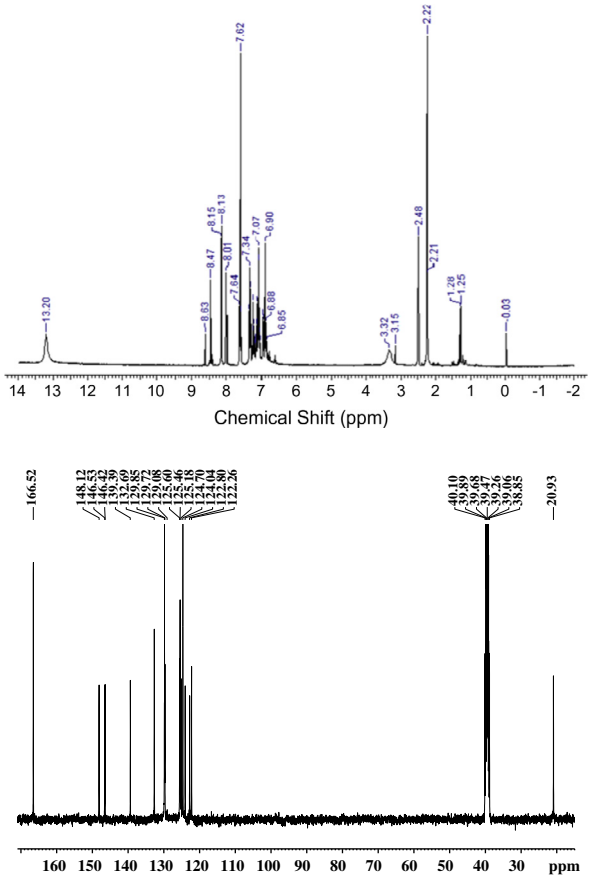

Fig. 3. ^{1}H and ^{13}C NMR spectrum of MePIFA in DMSO solution.

observed as a medium band at 1321 cm^{-1} in the FT-IR. But out-of-plane bending vibration of the molecule was calculated as 591, 636 cm^{-1} and it was observed at 642 cm^{-1} as a very weak band in the FT-IR and at 640 cm^{-1} in dispersive Raman. Observed wavenumbers show good agreement with the calculated wavenumbers.

CH_3 vibrations

The MePIFA molecule has one CH_3 group. The C—H stretching of CH_3group are expected to be at lower frequencies than those of aromatic ring (3100–3000 cm^{-1}). The asymmetric stretch is usually observed at higher wavenumber than the symmetric stretch. Methyl group vibrations are generally referred as electron-donating substituent in the aromatic rings system. The asymmetric C—H stretching mode of CH_3 is expected around 2980 cm^{-1} and symmetric C—H stretching mode of CH_3 should beat 2870 cm^{-1} from previous works in the literature [37,39–41]. In the present work, asymmetric stretching vibration of CH_3 were calculated at 3002 and 2977 cm^{-1} with B3LYP method and they it was observed at 2863 cm^{-1}in the FT-IR spectrum. On the other hand, the CH_3 symmetric stretching vibration was calculated at 2924 cm^{-1} but it was observed at 2656 cm^{-1} in FT-IR spectrum and at 2918 cm^{-1} in dispersive Raman. These vibrations show more than 99% of PED contribution suggesting that it is a pure stretching mode. Scissoring vibrations of CH_3 were calculated at 1441 and 1442 cm^{-1} with B3LYP/6-311G(d,p) method with PED contribution of more than 40%.

C—H vibrations

The hetero aromatic structures have always C—H stretching vibrational modes as weak bands in the region between 3000 and 3100 cm^{-1} [35,42–44]. The MePIFA molecule has 12 C—H moiety in the aromatic ring systems. For MePIFA molecule, the C—H stretching vibration computed in the range of 3060–3135 cm^{-1} with the B3LYP/6-311G(d,p) method were observed at 3033 cm^{-1} in FT-IR and at 3061 and 3185 cm^{-1} in dispersive Raman. The C—H in-plane bending vibrational modes appear in the range of 1000–1300 cm^{-1} in the literature [45,46]. The C—H in-plane bending vibrations observed at 1166 cm^{-1} in FT-IR and at 1060, 1218 cm^{-1} in dispersive Raman spectrum, were calculated in range of 1015–1255 cm^{-1} for MePIFA. The C—H out-of-plane bending vibration is shown in the range of 800–950 cm^{-1} for aromatic compounds in the literature [45,46]. The C—H out of plane bending vibrations were calculated in range of 818–964 cm^{-1} for MePIFA. These vibrational modes were observed at 902 and 935 cm^{-1} in FT-IR and at 950 cm^{-1} in dispersive Raman spectrum. The predicted values show good agreement with the recorded spectrum as in Table 1.

C—N

The C—N stretching vibration was assigned in the region between 1382 and 1266 cm^{-1} for aromatic amines in the literature [47–49]. The assignment of the C—N and C=N vibrations is not easy since separation of these vibrations from each other is difficults. These vibrations were calculated in the range of 1289–1255 cm^{-1}. The same vibration was observed at 1273 cm^{-1} in FT-IR and at 1292 cm^{-1} in dispersive Raman spectrum. The theoretically predicted scaled results show good agreement with the experimental data. The PED of this vibration suggests that C—C stretching vibration has a mixed mode.

NBO analysis

In quantum chemistry, a natural bond orbital or NBO is a computed bonding orbital with maximum electron density. Natural bond orbitals are used in computational chemistry to calculate bonds and the distribution of electron density between atoms. NBO provides the most accurate possible "natural Lewis structure"

Table 4
Comparison of experimental (in DMSO, water and gas solutions) and calculated absorption wavelength (λ, nm), excitation energies (E, eV) and oscillator strengths (f) of MePIFA.

Experimental		TD-B3LYP/6-311G(d,p)			CIS/6-311G(d,p)		
λ (nm)	E (eV)	λ (nm)	E (eV)	f	λ (nm)	E (eV)	f
DMSO							
392.28	3.164	430.31 (91 → 92)	2.8813	0.0179	259.56 (91 → 92)	4.7767	0.1391
300.85	4.136	353.75 (91 → 93)	3.5049	0.2063	240.22 (86 → 92) (91 → 93) (91 → 105)	5.1612	0.2821
235.46	5.270	300.56 (91 → 94)	4.1252	0.2302	227.44 (87 → 94) (88 → 96) (91 → 94)	5.4513	0.3587
Water							
		430.15 (91 → 92)	2.8823	0.0171	258.93 (91 → 92)	4.7883	0.1256
		353.22 (91 → 93)	3.5101	0.1985	239.46 (86 → 92) (91 → 93) (91 → 105)	5.1777	0.2570
		300.12 (90 → 92) (91 → 94)	4.1311	0.2171	226.75 (87 → 94) (88 → 96) (91 → 94)	5.4680	0.3267
Gas							
		419.98 (91 → 92)	2.9522	0.0137			
		344.09 (91 → 93)	3.6033	0.1678			
		299.09 (91 → 94)	4.1454	0.1534			

picture of ψ, because all orbital details are mathematically chosen to include the highest possible percentage of the electron density (ED). The bonding NBOs are of the Lewis orbital type (occupation numbers near 2); antibonding NBOs are of the non-Lewis orbital type (occupation numbers near 0). Full Lewis orbitals with two electrons were complemented by formally empty non-Lewis orbitals [50]. Delocalization of electron density between occupied Lewis-type (bond or lone pair) NBO orbitals and formally unoccupied (anti-bond or Rydberg) non-Lewis NBO orbitals correspond to a stabilizing donor–acceptor interaction. The interactions result is a loss of occupancy from the localized NBO of the idealized Lewis structure into an empty non-Lewis orbital. For each donor (i) and acceptor (j), the stabilization energy E(2) associated with the delocalization $i \rightarrow j$is estimated as

$$E_2 = \Delta E_{ij} = q_i \frac{F(i,j)^2}{\epsilon_j - \epsilon_i} \quad (2)$$

where q_i is the donor orbital occupancy, ε_i and ε_j are diagonal elements and F(i,j) is the off diagonal NBO Fock matrix element [51].

The NBO calculation was performed using Gaussian 09 package at the DFT/B3LYP level for MePIFA and the corresponding results were given in Table 2. The intramolecular interactions were observed as an increase in electron density (ED) in (C—C) antibonding orbital that weakens the related bonds. The electron density of conjugated bonds of aromatic ring (1.97e) was clearly demonstrated a strong delocalization for MePIFA molecule. The occupancy of π bonds is lesser than σ bonds which lead more delocalization.

The intramolecular hyperconjugative interactions of the σ (C16—C20) distributed to σ^* (C14—C16), (C18—C20) leads to less stabilization of 3.87, 3.44 kJ/mol for MePIFA. These have enhanced further to conjugate with antibonding orbital of π^* (C13—C14), (C15—C18) which leads to strong delocalization of 20.05, 22.90 kJ/mol. The same kind of interaction was computed as C2—C4, C13—C14, C23—C24, C25—C28 and C26—C30 bonds as shown in Table 2. The other important interaction is the π^* (C13—C14) bond conjugated to the π^* (C16—C20) showing enormous stabilization energy of 273.40 kJ/mol for MePIFA.

NMR analysis

After optimization of molecule, ^{13}C and ^{1}H NMR chemical shifts calculations were carried out by using B3LYP with 6-311G(d,p) basis set with the GIAO method [52,53].These calculations were performed in DMSO, water and gas phase. Chemical shifts calculated in the DMSO solution are in good agreement with the experimental chemical shifts obtained from DMSO solution. Calculated and experimental chemical shift of molecule in ^{13}C and ^{1}H NMR spectrum are given in the Table 3. The measured ^{13}C and the ^{1}H NMR spectra are shown in Fig. 3.

^{1}H NMR chemical shift values calculated in DMSO and water (with respect to TMS) are in the range of 2.03–8.29 ppm and in the range of 1.96–8.27 ppm for the gas phase. Experimental shifts of the solutions prepared in DMSO are observed in the range of 0.03–13.20 ppm. Chemical shifts with aromatic protons were calculated theoretically in the range of 6.95–8.29 ppm in DMSO and water, in the range of 6.88–8.27 ppm for the gas phase of MePIFA. This chemical shift experimentally was observed in the range of 6.85–8.63 ppm in DMSO. The calculated chemical shifts of proton NMR are in good agreement with experimental values.

Aromatic carbons give signals in overlapped areas of the spectrum with chemical shift values from 100 to 150 ppm [54,55]. In this work, the aromatic carbons signals were obtained in the range of 155.72–126.10 ppm for DMSO and water solutions and in the range of 155.23–126.28 ppm in the gas phase. The experimental values for aromatic carbons were observed in the range of 166.52–122.26 ppm.

UV–VIS analysis

Electronic absorption spectra were calculated with TD-DFT and CIS methods based on the B3LYP/6-311G(d,p) level for an optimized structure in DMSO, water and gas phase for MePIFA molecule. The calculated absorption wavelengths (λ), excitation energies (E) and oscillator strengths (f) were carried out and compared with experimental values listed in Table 4. These bands for MePIFA were obtained at 430.31, 353.75 and 300.56 in DMSO, at 430.15, 353.22 and 300.12 in water, at 419.98, 344.09 and 299.09 in gas phase for TD-DFT and at 259.56, 240.22 and 227.44 in DMSO and at 258.93, 239.46 and 226.75 in water for CIS. But, in gas phase calculated with CIS methods of MePIFA molecule did not recorded any value. The experimental and theoretical electronic absorption spectra taken in DMSO for the title compound are given in Fig. 4. The electronic absorption spectra shows three bands at 235.46, 300.85 and 386.48 in DMSO.

Total, partial and population density of states (DOS, PDOS and OPDOS) spectra analysis

To ensure an illustrated representation of molecule orbital(MO) compositions, the TDOS, PDOS, and OPDOS or COOP density of

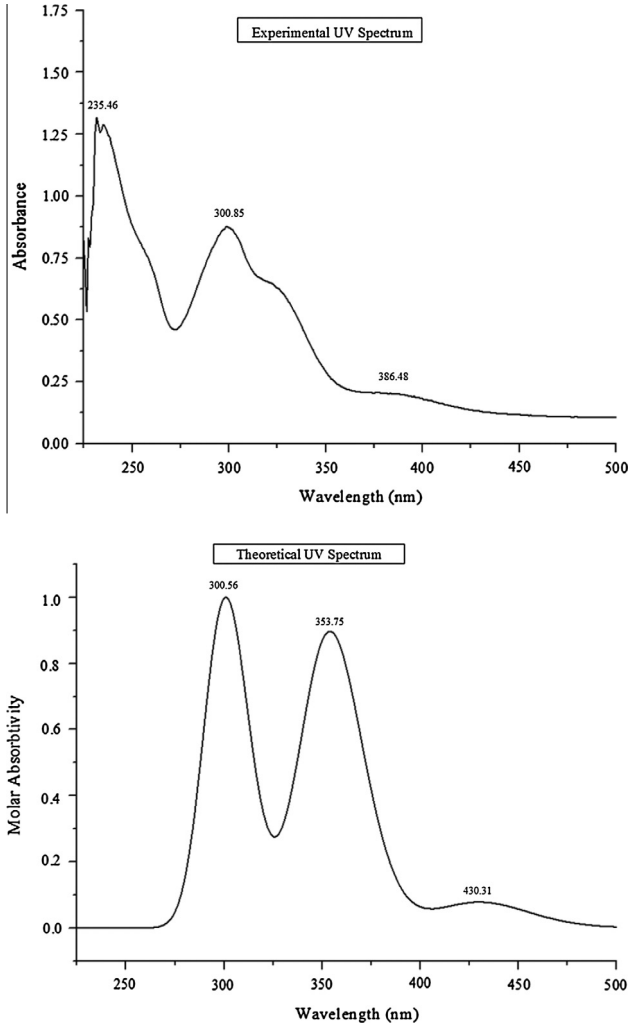

Fig. 4. The experimental and theoretical UV–Vis spectrum of MePIFA for DMSO solutions.

states of MePIFA were plotted in Fig. 2. The full width at half maximum (FWHM) of 0.3 eV with the GaussSum 2.2 program [20] were obtained with by convoluting the molecular orbital information with Gaussian curves of unit height. Atoms were divided three groups. Methyl group (CH_3^-) was taken into phenyl groups because of no charge density. The most important application of the DOS spectra is to show MO compositions and their contributions to chemical bonding through the OPDOS spectra. Positive value of the OPDOS shows a bonding interaction, but negative value shows anti-bonding interaction and zero value shows nonbonding interactions [56].

As seen in Fig. 7, HOMO orbitals are localized on the phenyl rings and nitrogen atom and LUMO orbitals are localized on the ring and carboxyl group of MePIFA. The OPDOS diagram is shown in Fig. 5. Some of orbital energy values of interaction between selected groups, such as phenyl ring ↔ carboxyl groups (red line) system are positive (bonding interaction). However, phenyl ring ↔ nitrogen atoms (blue line) have bonding and anti-bonding character.

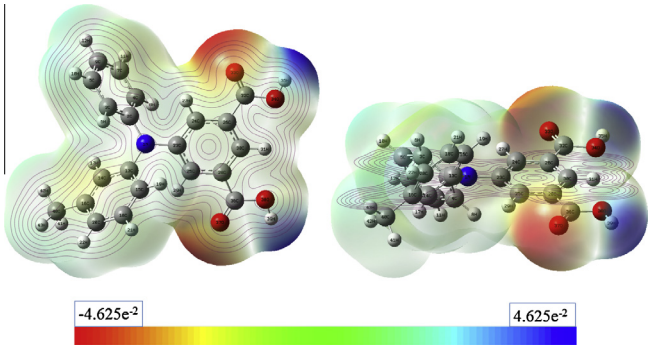

Fig. 6. Molecular electrostatic potential map of MePIFA.

Molecular electrostatic potential surface

Fig. 6 shows 3D plots of molecular electrostatic potential (MEP) map with constant electron density surface of MePIFA. The MEP is

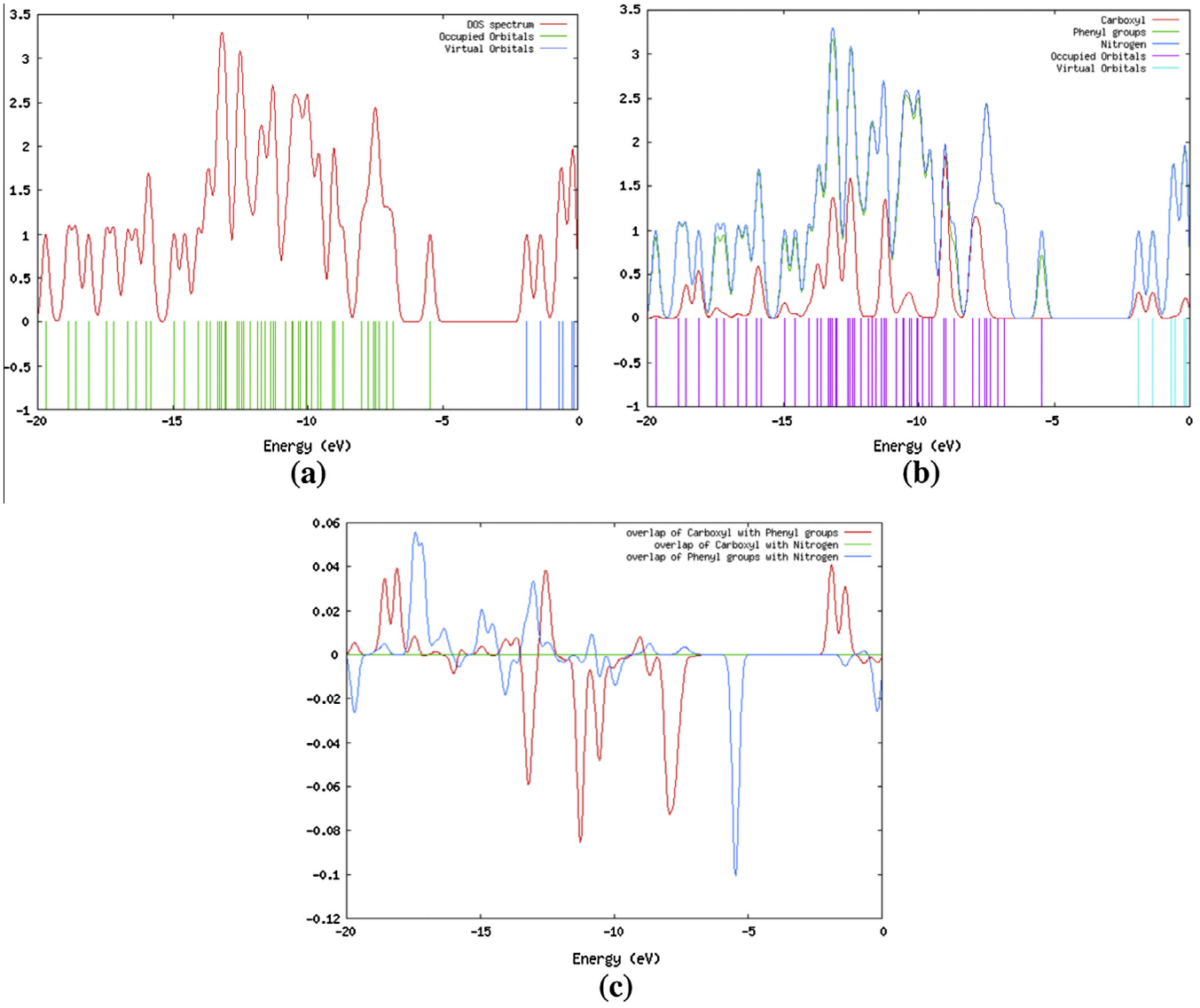

Fig. 5. (a) The calculated total electronic density of states diagrams for MePIFA, (b) the calculated partial electronic density of states diagrams for MePIFA and (c) the overlap population electronic density of states diagrams for MePIFA.

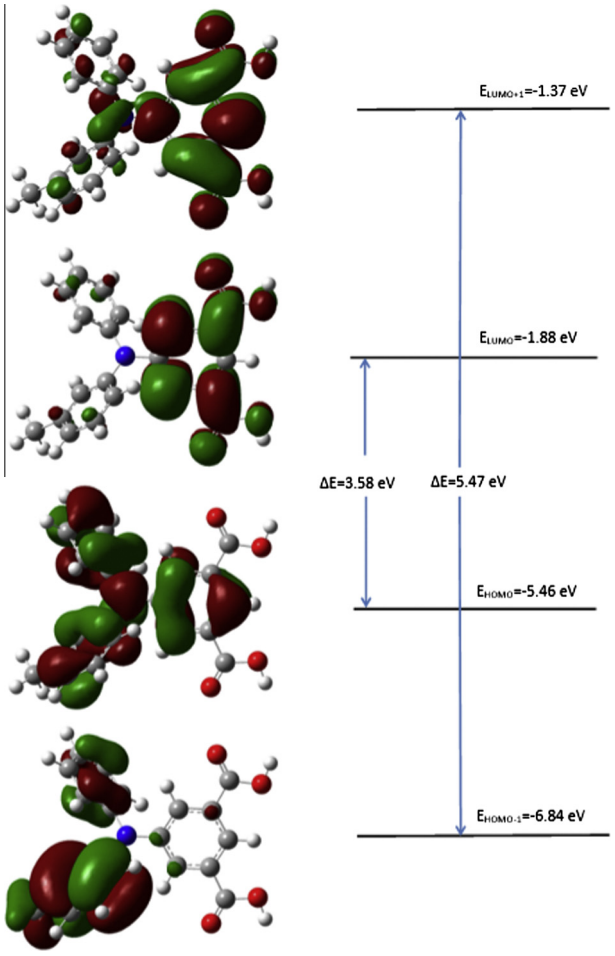

Fig. 7. The frontier molecular orbitals of MePIFA for gas phase.

a useful feature to study reactivity for approaching electrophile. It will be attracted by negative regions (where the electron distribution effect is dominant). Plot of the MEPs, while the maximum negative region which preferred site for electrophilic attack indications as red color, the maximum positive region which preferred site for nucleophilic attack symptoms as blue color. The importance of MEP map simultaneously displays molecular size, shape as well as positive, negative and neutral electrostatic potential regions in terms of color grading. It is very useful in research of molecular structure with its physiochemical property relationship [57–60].

The different values of the electrostatic potentials at the surface are represented with different colors in the map of MEPs. The potential increases change from red to blue color. The color code maps are in the range between −0.04625 (dark red) and 0.04625 a.u. (dark blue) in compound, where blue indicates the strongest attraction and red indicates the strongest repulsion. The regions having the negative potential are over the oxygen atoms (O_{33} and O_{37}) while regions having the positive potential are near OH groups for MePIFA. The results show that the H_{35} and H_{39} atoms indicate the strongest attraction and O_{33} and O_{37} atoms indicating the strongest repulsion.

HOMO–LUMO analysis

The HOMO represents the orbitals with the ability of donating electrons, while LUMO behaves as an electron acceptor with the ability of collecting excited electron from HOMO. The total energy, energy gap and dipole moment affect the stability of a molecule. Surfaces of the frontier orbital were drawn to understand the bonding scheme of present compound. The HOMO and LUMO energy levels were calculated with TD-DFT/B3LYP/6-311G(d,p) method in DMSO, water and gas phase. The calculated energy values are given in Table 5. Plots of the HOMO − 1, HOMO, LUMO and LUMO + 1orbitals for the title molecule were shown for gas phase in Fig. 7. HOMO orbitals are localized on the phenyl rings and nitrogen atom and LUMO orbitals are localized on the ring and carboxyl group of MePIFA. The energy difference between H → L and H−1 → L + 1 orbital is a critical parameter to determine molecular electrical transport properties, because it is a measure of electron conductivity. The energy difference between HOMO and LUMO levels are 3.52 eV in DMSO and water, but it is 3.58 eV in gas phase for MePIFA.

The chemical harness is 1.76 eV in DMSO and water, but is 1.79 eV in gas phase for MePIFA as shown in Table 5. The values of electronegativity, chemical potential and electrophilicity index of MePIFA are also given Table 5.

Experimental Electrochemical properties

The experimental HOMO–LUMO values for MePIFA were calculated from cyclic voltammtery. The cyclic voltammograms are given in Fig. 8, the MePIFA molecule shows one reversible oxidation peak attributed to the tri-arylamine moieties of this compound. This compound consist of irreversible reduction peaks attributed to carboxylic acid anchoring acceptor units. The oxidative potential values are 1.21 V for MePIFA. The reduction potential values are obtained as −1.46 V. HOMO and LUMO levels of MePIFA were calculated from their oxidation and reduction potential values. HOMO levels are calculated as −5.61 eV, while LUMO levels are −2.94 eV. The calculated gas-phase HOMO and LUMO values are very close to the experimental values.

Table 5
The calculated energies values of MePIFA using by the TD-DFT/B3LYP method using 6-311G(d,p) basis set.

MePIFA	Gas	DMSO	Water
E_{total} (Hartree)	−1166.35681722	−1166.47934619	−1166.47954738
E_{HOMO} (eV)	−5.46	−5.56	−5.56
E_{LUMO} (eV)	−1.88	−2.04	−2.04
E_{HOMO-1} (eV)	−6.84	−6.91	−6.91
E_{LUMO+1} (eV)	−1.37	−1.53	−1.54
$E_{HOMO-1-LUMO+1\ gap}$ (eV)	5.47	5.38	5.37
$E_{HOMO-LUMO\ gap}$ (eV)	3.58	3.52	3.52
Chemical hardness (h)	−1.79	−1.76	−1.76
Electronegativity (χ)	3.67	3.80	3.80
Chemical potential (μ)	−3.67	−3.80	−3.80
Electrophilicity index (ω)	−3.76	−4.10	−4.10

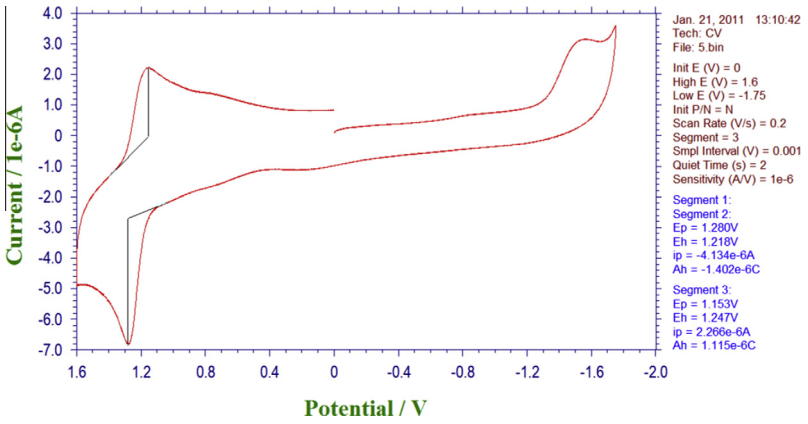

Fig. 8. Cyclic voltammograms of the MePIFA.

Conclusion

The 5-[(3-methylphenyl) (phenyl) amino] isophthalic acid (MePIFA) molecule was characterized by FT-IR and FT-Raman spectra, NBO analysis, UV–Vis spectral analysis, HOMO–LUMO energy and ^{1}H and ^{13}C NMR spectroscopy. The geometry was optimized by using DFT/B3LYP method with 6-311G(d,p) basis sets. Scaling factor of 0.967 was used to fit the calculated wavenumbers with experimental wavenumbers. ^{1}H and ^{13}C chemical shifts were compared with experimental values in DMSO solution and showing a good agreement. Absorption wavelengths for the title molecule were calculated and compared with experimental UV–Vis spectra. DFT calculations carried out for MePIFA molecule, showed a good agreement with experimental values. The results show that there is an increase in the HOMO level of the MePIFA molecule, that suggest to be used as self-assembled monolayer films between ITO and organic hole transport layer in OLEDs.

Acknowledgements

This work was supported by TUBITAK under Grant No. TBAG-108T718 and by Ahi Evran University Scientific Project Unit (BAP) with, Project No: PYO-FEN.4003-12.009.

Appendix A. Supplementary material

Supplementary data associated with this article can be found, in the online version, at http://dx.doi.org/10.1016/j.saa.2014.05.021.

References

[1] C. Adachi, S. Tokito, T. Tsutsui, S. Saito, Jpn. J. Appl. Phys. 27 (1988) L269.
[2] S. Heum, P.M. Borsenberger, Chem. Phys. 200 (1995) 245.
[3] R.H. Young, J.J. Fitzgerald, J. Phys. Chem. 99 (1995) 4230.
[4] J. Kido, M. Kimura, K. Nagai, Science 267 (1995) 1332.
[5] V. Bulović, G. Gu, P.E. Burrows, S.R. Forrest, M.E. Thompson, Nature 380 (1996) 29.
[6] D.F. O'Brien, P.E. Burrows, S.R. Forrest, B.E. Koene, D.E. Loy, M.E. Thompson, Adv. Mater. 10 (1998) 1108.
[7] C. Ganzorig, M. Fujihira, Appl. Phys. Lett. 77 (2000) 4211.
[8] C. Ganzorig, K. Suga, M. Fujihira, Chem. Lett. 29 (2000) 1032.
[9] P. Strohriegl, J.V. Grazulevicius, Adv. Mater. 14 (2002) 1439.
[10] P.T. Furuta, L. Deng, S. Garon, M.E. Thompson, J.M.J. Fréchet, J. Am. Chem. Soc. 126 (2004) 15388.
[11] K. Sakanoue, M. Motoda, M. Sugimoto, S. Sakaki, J. Phys. Chem. A 103 (1999) 5551.
[12] M. Malagoli, J.L. Brédas, Chem. Phys. Lett. 327 (2000) 13.
[13] B.C. Lin, C.P. Cheng, Z.P.M. Lao, J. Phys. Chem. A 107 (2003) 5241.
[14] T. Sato, K. Shizu, T. Kuga, K. Tanaka, H. Kaji, Chem. Phys. Lett. 458 (2008) 152.
[15] J. Cornil, N.E. Gruhn, D.A. dos Santos, M. Malagoli, P.A. Lee, S. Barlow, S. Thayumanavan, S.R. Marder, N.R. Armstrong, J.L. Brédas, J. Phys. Chem. A 105 (2001) 5206.
[16] M. Malagoli, M. Manoharan, B. Kippelen, J.L. Brédas, Chem. Phys. Lett. 354 (2002) 283.
[17] H. Kaji, T. Yamada, N. Tsukamoto, F. Horii, Chem. Phys. Lett. 401 (2005) 246.
[18] C.W. Tang, S.A. Van Slyke, Appl. Phys. Lett. 51 (1987) 913–915.
[19] C.W. Tang, S.A. Van Slyke, C.H. Chen, J. Appl. Phys. 65 (1989) 3610.
[20] N.M. O'Boyle, A.L. Tenderholt, K.M. Langner, J. Comp. Chem. 29 (2008) 839–845.
[21] M. Can, A.K. Havare, H. Aydın, N. Yagmurcukardes, S. Demic, S. Icli, S. Okur, Submitted Appl. Surf. Sci. (submitted for publication).
[22] G. Keresztury, S. Holly, J. Varga, G. Besenyei, A.Y. Wang, J.R. Durig, Spectrochim. Acta 1993 (2007) 49A.
[23] G. Keresztury, J.M. Chalmers, P.R. Griffith (Eds.), Raman Spectroscopy: Theory, Hand book of Vibrational Spectroscopy, vol. 1, John Wiley & Sons Ltd., New York, 2002.
[24] M.H. Jamroz, Vibrational Energy Distribution Analysis, VEDA 4 Computer Program, Poland, 2004.
[25] E.D. Glendening, A.E. Reed, J.E. Carpenter, F. Weinhold, NBO Version 3.1, TCI, University of Wisconsin, Madison, 1998.
[26] M.J. Frisch, et al., Gaussian 09, Revision A.1, Gaussian Inc., Wallingford, CT, 2009.
[27] A.N. Sobolev, V.K. Belsky, I.P. Romm, N.Yu. Chernikova, E.N. Gurianova, Acta Crytallogr. C41 (1985) 967.
[28] Y. Erdogdu, M.T. Güllüoğlu, M. Kurt, J. Raman Spectrosc. 40 (2009) 1615–1623.
[29] Y.M. Wu, C.C. Dong, S. Liu, H.J. Zhu, Y.Z. Wu, Acta Crystallogr., Sect. E, Struct. Rep. E62 (2006) 4236.
[30] G. Varsanyi, Assignments of Vibrational Spectra of Seven Hundred Benzene Derivatives, vols. 1–2, Adam Hilger, 1974.
[31] D.L. Vein, N.B. Colthup, W.G. Fateley, J.G. Grasselli, The Handbook of Infrared and Raman Characteristic Frequencies of Organic Molecules, Academic Press, San Diego, 1991.
[32] B.H. Stuart, Infrared Spectroscopy: Fundamentals and Applications, John Wiley & Sons, England, 2004.
[33] S. Chandra, H. Saleem, N. Sundaraganesan, S. Sebastian, Spectrochim. Acta A74 (2009) 704.
[34] R.M. Silverstein, F.X. Webster, Spectroscopic Identification of Organic Compound, sixth ed., John Willey & Sons, New York, 1998.
[35] G. Varsanyi, Vibrational Spectra of Benzene Derivatives, Academic Press, New York, 1969.
[36] A. Poiyamozhi, N. Sundaraganesan, M. Karabacak, O. Tanrıverdi, M. Kurt, J. Mol. Struct. 1024 (2012) 1–12.
[37] G. Socrates, Infrared Characteristic Group Frequencies, John Wiley and Sons, New York, 1980.
[38] Y. Shirota, K. Okumoto, H. Inada, Synth. Met. 111 (2000) 387.
[39] D.A. Kleinman, Phys. Rev. 1962 (1977) 126.
[40] N.B. Colthup, L.H. Daly, S.E. Wiberly, Introduction to Infrared and Raman Spectroscopy, Academic Press, New York, 1990.
[41] B. Venkataram Reddy, G. RamanaRao, Vib. Spectrosc. 6 (1994) 231.
[42] V. Krishnakumar, V. Balachandran, T. Chithambarathanu, Spectrochim. Acta 62A (2005) 918.
[43] N. Puviarasan, V. Arjunan, S. Mohan, Turk. J. Chem. 26 (2002) 323.
[44] V. Krishnakumar, R. John Xavier, Indian J. Pure Appl. Phys. 41 (2003) 597.
[45] V. Krishnakumar, V.N. Prabavathi, Spectrochim Acta, Part A 71 (2008) 449.
[46] A. Altun, K. Golcuk, M. Kumru, J. Mol. Struct. 637 (2003) 155.
[47] A. Usha Rani, N. Sundaraganesan, M. Kurt, M. Cinar, M. Karabacak, Spectrochim. Acta A 75 (2010) 1523–1529.
[48] M. Karabacak, M. Kurt, M. Cınar, A. Coruh, Mol. Phys. 107 (2009) 253–264.
[49] M. Karabacak, M. Cinar, Z. Unal, M. Kurt, J. Mol. Struct. 982 (2010) 22–27.
[50] F. Weinhold, C.R. Landıs, Chem. Educ. Res. Pract. Europe 2 (2) (2001) 91–104.
[51] A.E. Reed, L.A. Curtiss, F. Weinhold, Chem. Rev. 88 (1988) 899.
[52] R. Ditchfield, J. Chem. Phys. 56 (1972) 5688–5691.

[53] K. Wolinski, J.F. Hinton, P. Pulay, J. Am. Chem. Soc. 112 (1990) 8251–8260.
[54] H.O. Kalinowski, S. Berger, S. Braun, Carbon-13 NMR Spectroscopy, John Wiley & Sons, Chichester, 1988.
[55] K. Pihlaja, E. Kleinpeter (Eds.), Carbon-13 chemical shifts in structural and stereochemical analysis, VCH Publishers, Deerfield Beach, 1994.
[56] M. Chen, U.V. Waghmare, C.M. Friend, E. Kaxiras, J. Chem. Phys. 109 (1998) 6680–6854.
[57] J.S. Murray, K. Sen, Molecular Electrostatic Potentials, Concepts and 399 Applications, Elsevier, Amsterdam, 1996.
[58] E. Scrocco, J. Tomasi, in: P. Lowdin (Ed.), Advances in Quantum Chemistry, Academic Press, New York, 1978, p. 402.
[59] J. Sponer, P. Hobza, Int. J. Quant. Chem. 57 (1996) 959–970.
[60] F.J. Luque, M. Orozco, P.K. Bhadane, S.R. Gadre, J. Phys. Chem. 97 (1993) 9380–9384.